Analytical note

New insights on the Dronino iron meteorite by double-pulse micro-Laser-Induced Breakdown Spectroscopy

Gioacchino Tempesta[a],[*], Giorgio S. Senesi[b], Paola Manzari[c], Giovanna Agrosì[a]

[a] *Dipartimento di Scienze della Terra e Geoambientali (DiSTeGeo), University of Bari, Via E. Orabona 4, 70125 Bari, Italy*
[b] *CNR – Istituto di Nanotecnologia (NANOTEC), PLasMI Lab, Via Amendola 122/D, 70126 Bari, Italy*
[c] *Istituto Nazionale di Astrofisica, Istituto di Astrofisica e Planetologia Spaziali (INAF-IAPS), via Fosso del Cavaliere 100, Roma, Italy*

ARTICLE INFO

ABSTRACT

Two fragments of an iron meteorite shower named Dronino were characterized by a novel technique, i.e. Double-Pulse micro-Laser Induced Breakdown Spectroscopy (DP-µLIBS) combined with optical microscope. This technique allowed to perform a fast and detailed analysis of the chemical composition of the fragments and permitted to determine their composition, the alteration state differences and the cooling rate of the meteorite. Qualitative analysis indicated the presence of Fe, Ni and Co in both fragments, whereas the elements Al, Ca, Mg, Si and, for the first time Li, were detected only in one fragment and were related to its post-falling alteration and contamination by weathering processes. Quantitative analysis data obtained using the calibration-free (CF) - LIBS method showed a good agreement with those obtained by traditional methods generally applied to meteorite analysis, i.e. Electron Dispersion Spectroscopy - Scanning Electron Microscopy (EDS-SEM), also performed in this study, and Electron Probe Microanalysis (EMPA) (literature data). The local and coupled variability of Ni and Co (increase of Ni and decrease of Co) determined for the unaltered portions exhibiting plessite texture, suggested the occurrence of solid state diffusion processes under a slow cooling rate for the Dronino meteorite.

© 2017.

1. Introduction

The study of meteorites can provide unique information on the chemical composition of the solar system since it was born and details on how it evolved into the Sun and planets of today. The information that can be obtained goes back until to 4.6 billion years. Among the known meteorites, those classified as iron and stony-iron consist of asteroid fragments that were subjected to significant geological processing in the early solar system, including melting of metals and silicates and differentiation into core, mantle and crust. However, after falling the body of these meteorites experienced also a geological evolution typical of that occurring on the Earth, but at a much smaller intensity and timescale [1]. Meteorites represent the only available material analogues to those present in the deep interiors of Earth and other solar planets, so the discrimination between fragments that suffered terrestrial alteration and unaltered samples can be relevant for genetic implications [1].

In the last decades, a novel, highly versatile advanced analytical technique, i.e. Laser-Induced Breakdown Spectroscopy (LIBS) has been widely and successfully applied to the study of various types of terrestrial and extraterrestrial materials in the solid, liquid or gaseous phase [2]. LIBS shows great advantages, such as no need of sample preparation, possibility of simultaneous multi-element analysis, fast response, capacity of performing depth-profile analysis based on a simple set-up, and availability of portable instruments suitable for applications in harsh environments [3–5]. In the last years, many space agencies programs concerning Mars exploration have shown a great interest on the application of LIBS to the analytical study of Mars rocks and soils. In particular, a stand-off LIBS system has been deployed on the Mars rover Curiosity as a part of the ChemCam analytical system that is presently used to study the geochemistry of the Martian surface (NASA 2016) [6].

The LIBS technique has already been tested successfully for meteorite characterization in a number of previous works [7–13] that, in general, have shown that the higher was the concentration of elements, the better was the agreement with data obtained by other techniques. Further, little differences of the minor element presence and content might play a fundamental role for meteorite classification.

In this study two fragments of an iron meteorite shower named Dronino were studied using a non-conventional technique, i.e. double-pulse micro-Laser-Induced Breakdown Spectroscopy (DP-µLIBS) in conjunction with optical microscope, which allowed to obtain a fast multi element quantitative analysis also of light elements. Dronino meteorite was discovered by Oleg Guskov in the year 2003 near the village of Dronino in the Ryazan oblast, Russia [14]. After this finding, scientific expeditions and meteorite hunters collected more than 600 fragments (the largest of 250 kg) totaling about 3000 kg, which were found at a depth of 0.2–2 m across an area of

0.5×1.5 km. The distribution of fragments suggested that the meteorite formed a crater of about 30 m in diameter, which was probably buried. Since no historical records of a meteorite fall exist, it is likely that the meteorite fell before the 12th century when the area was largely unpopulated [15]. According to Russell et al. [15], the bulk composition of the Dronino meteorite consisted of fine-grained ataxitic duplex texture containing kamacite (7.0 ± 0.5 wt% Ni and 0.75 wt% Co) and taenite (26.3 ± 0.5 wt% Ni and 0.35 wt% Co).

Successively, this meteorite has been studied extensively to investigate the alteration processes that affected its mineralogy and bulk chemistry. Most fragments of Dronino appeared strongly oxidized, although some metal with massive sulfide inclusions was still non–oxidized in larger samples [16]. In a Mössbauer spectroscopy and X-ray diffraction study of the metal portion of the meteorite Grokhovsky et al. [16] found that Dronino consisted mainly of large kamacite grains (20–80 μm in size) of irregular shape dispersed in the matrix and contained about 10 vol% of rounded, often elongated sulfide nodules of a few mm in size, with occasional small worm-like sulfide inclusions. These nodules consisted of troilite that in some cases appeared partially or totally replaced by Fe/Ni sulfides formed under terrestrial alteration. All nodules appeared surrounded by Fe hydroxides that replaced the metal, whereas some troilite nodules contained rare tiny metal grains with 52–53 wt% Ni. Accessory minerals found in Dronino were chromite and Fe phosphate. Chromite occurred commonly as small euhedral crystals included in sulfide nodules and contained MnO (0.2–0.4 wt%), TiO_2 (0.2 wt%), and V_2O_3 (0.2–0.5 wt%). Minute chromite inclusions were also found in Fe phosphate, whereas no phosphides were detected, and no P content was detectable by Electron Probe Microanalysis (EMPA) in the metal.

More recently, Yakovlev et al. [17] studied, also by X-ray diffraction and Mössbauer spectroscopy the weathering products of two Dronino fragments found the one in a wet and the other in a dry clay sand. Two types of alteration consisting in an internal and an external surface layer were found in both fragments. In particular, the weathering products in the fragment collected in the wet clay sand consisted of magnetite (Fe_3O_4), maghemite (γ-Fe_2O_3), goethite (α-FeOOH) and probably ferrihydrite ($5Fe_2O_3$-$9H_2O$), whereas those in the fragment collected in the dry clay sand were ferric hydrous oxides (FeOOH) and siderite ($FeCO_3$).

In this study new data on the compositional and mineralogical characteristics of the Dronino meteorite allowed to distinguish altered from unaltered fragments, providing novel additional information on the geochemistry of the site where the meteorite fragments were found. Moreover, new insights about the cooling rates of the meteorite were inferred. The validity of LIBS quantitative compositional results was confirmed by comparing the LIBS data with those obtained by Electron Dispersion Spectroscopy - Scanning Electron Microscopy (EDS-SEM).

2. Materials and methods

2.1. Samples

Two fragments of the Dronino meteorite were examined in this study, i.e. fragment 1 with evident effects of alteration (Fig.1a) and fragment 2 featuring the original typical plessite texture and elongated sulfide inclusions characterized by a metallic luster (Fig.1b).

The two fragments investigated had their own certification that reported only the location, but not the specific site characteristics, i.e. the description of the geo-pedological settings where the fragments were found and collected. However, by comparing these samples with the fragments of Dronino meteorite studied by Yakoklev et al. [17] and accordingly with the results obtained in this previous paper, fragment 1 could be related to a sandy, permeable, water-bearing soil (a wet clay sand), and fragment 2 to a drier site. Due to the evident weathering layer (rusty aspect) covering fragment 1, a portion of it was previously cleaned off the weathered layer, and both original and polished samples were analyzed and characterized comparatively.

2.2. The LIBS experiment

A Nd:YAG Q-Switch LIBS system (Modì, Marwan) generating two laser beams in collinear geometry both at a laser wavelength of 1064 nm (IR) was used for the acquisition of the DP spectra. The DP mode, which consisted of two successive laser pulses temporally spaced of few ns or μs, was adopted to improve the LIBS signal intensity by coupling better the laser energy to the ablated target material in order to obtain a more efficient generation of analyte atoms in the excited state [2]. In the simplest collinear DP configuration used here the two laser beams had the same propagation pathway with the second pulse used to increase the amount of ablated material and, especially, reheat the plasma, so increasing its volume and emission. Further, the LIBS system was coupled by an objective lens ($10\times$ NA 0.25 WD 14.75 mm) to a petrographic optical microscope, which produced a spot of about 10–15 μm diffraction limited.

The DP-μLIBS analysis was performed using an energy value of 120 mJ by firing 5 consecutive laser shots on 4 points of the original (Fig. 1a) and polished (yellow circle in Fig. 2a) surfaces of fragment 1 and on 5 aligned points (red circle in Fig. 2b) of fragment 2.

The maximum repetition rate used was 10 Hz, and the delay time between the two laser pulses was fixed at 1 μs. The LIBS spectra were acquired with a delay of 2 μs after the second pulse, integrated for 2 ms, and then averaged. The plasma emission was collected us-
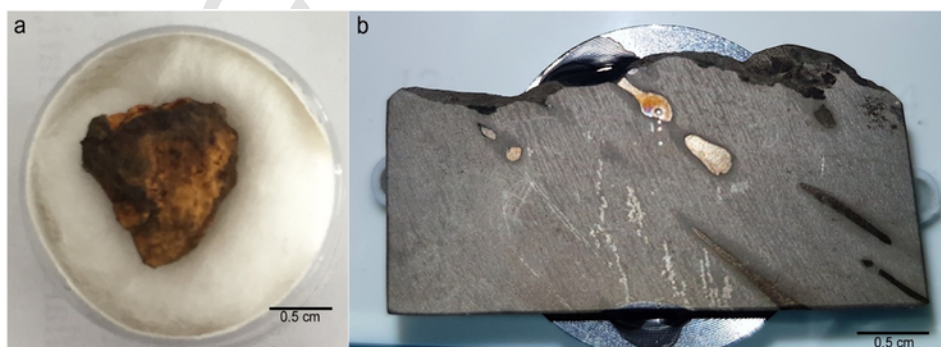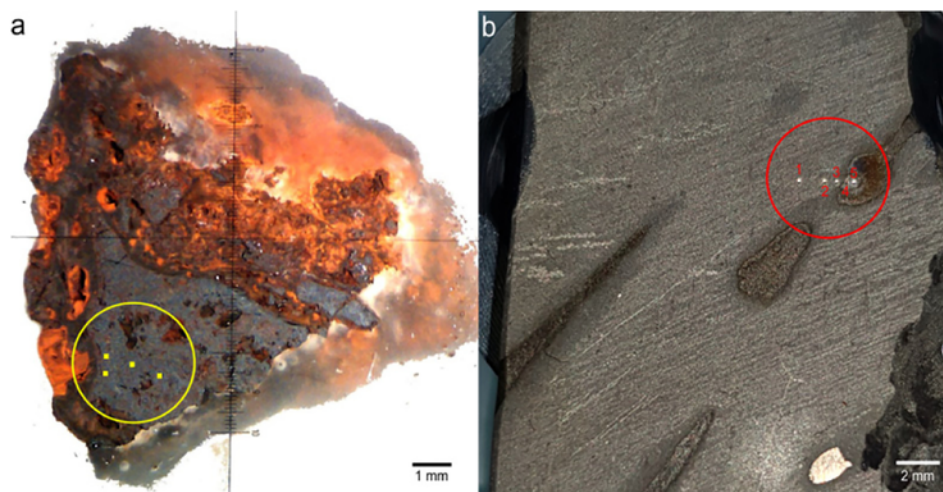

Fig. 1. Fragment 1 (a) and fragment 2 (b) of the Dronino iron meteorite.

Fig. 2. Areas analyzed on Dronino fragment 1: polished area (yellow circle) (a); spots analyzed on the cut surface of fragment 2(red circle) (b). (For interpretation of the references to colour in this figure legend, the reader is referred to the web version of this article.)

ing an optical fiber and the detection was performed by a double spectrometer Avantes (AvaSpec Dual-channel Fiber Optic Spectrometer), which covered simultaneously the spectral ranges 190–400 nm (with a spectral resolution of 0.2 nm) and 400–900 nm (with a resolution of 0.4 nm). The wavelength calibration was performed by using a spectral calibration lamp (AvaLight-CAL-Mini). After acquisition and storage the LIBS spectra were qualitatively and quantitatively analyzed using the calibration-free method (CF-LIBS) implemented by a proprietary software (LIBS++) [18]. The use of LIBS++ to perform CF-LIBS quantification implied that the plasma was in Local Thermodynamic Equilibrium (LTE) [19]. This was verified by calculating the value of plasma parameters, i.e. the electron density (N_e) obtained by the Stark broadening of the H line and excitation temperature (T_{ex}) by the Fe emission lines in the Boltzmann plot.

2.3. SEM-EDS measurements

The two fragments were studied chemically and morphologically by SEM using a SIGMA 300 VP Zeiss Sigma Field Emission instrument that operated in both high vacuum and variable pressure modes

at a resolution of ~10 nm. The instrument was equipped with secondary and backscattered electron (BSE) detectors, an in-lens electron detector, a cathodoluminescence (CL) detector, and a Bruker energy dispersion spectroscopy (EDS) system with dual silicon drift detectors, each of an area of 60 mm^2 and a resolution of 123 eV.

The EDS analysis was performed to measure the qualitative and quantitative chemical composition of the fragment mineralogical phases. The X-ray intensities were converted to wt% by the XPP correction method [20,21] using the quantitative Oxford software support. The accuracy of analytical data was also checked using several standard minerals manufactured by Micro-Analysis Consultants Ltd.

3. Results and discussion

3.1. Analysis of fragment 1

The DP-µLIBS averaged spectra of the unpolished and polished portions of fragment 1 surfaces were acquired in the spectral window 200–700 nm (Fig. 3). The spectra were normalized, overlapped and the background was reduced. The emission lines of Al, Ca, Co, Fe,
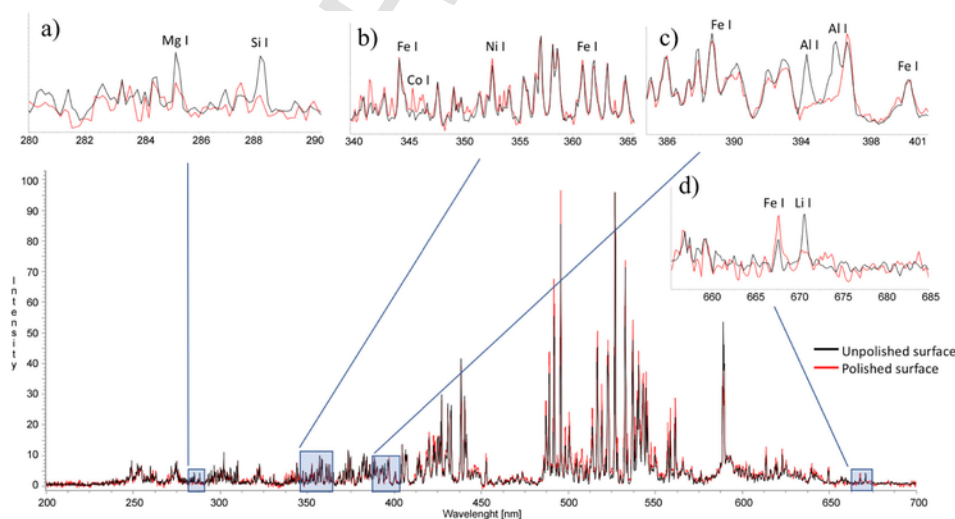
Fig. 3. DP-µLIBS spectra of the original and polished surfaces of fragment 1. Spectral windows: 280–290 nm (a); 340–365 nm (b); 385–400 nm (c); 650–665 nm (d).

Mg, Si, Ni and Li were identified in the spectra using the NIST database [22]. In particular, for the first time Li was detected in Dronino meteorite. The emission lines of Al, Ca, Mg, Li and Si were much more intense in the spectra acquired on the unpolished surface (Fig. 3), and their pervasive presence would exclude their origin from occasional surface contamination by sample handling.

The presence of Al, Ca, Mg and Si on the unpolished surface of fragment 1, which was confirmed also by EDS-SEM data, was indicative of minerals typical of clays and sands. In agreement with Yakovlev et al. [17], these results suggested the occurrence of terrestrial contamination during weathering. Further, the presence of Li might be related to the Li-rich water in the swamp where fragment 1 was collected. The Li content in alkaline environments has been reported previously [23,24].

To achieve information about the mineralogical composition, quantitative analyses of Fe, Ni and Co were performed by DP-μLIBS and EDS-SEM on the original and polished surfaces of fragment 1. The N_e ant T_{ex} values were measured to obtain by LIBS++ quantitative data. For fragment 1, the N_e measured was around $2.30 \cdot 10^{17}\,cm^{-3}$ with a variation of about 10–20%. The T_{ex} value obtained by the Boltzman plot (Fig. 4) was $7900 \pm 320\,K$ for all spots analyzed in all samples. Some slight deviations were due to differences in the ablation efficiency related to the surface condition of the iron meteorite.

A good agreement was apparent when comparing experimental CF-LIBS and EDS-SEM data with EMPA data from the literature by [15] (Table 1), which suggested an overall composition of kamacite.

To confirm the elemental composition of the polished surface, fragment 1 was also analyzed by BSE imaging and EDS X-ray mapping. The BSE image acquired on the polished surface (Fig. 5a) showed a thick altered rim (grey zone) and an unaltered area (white zone). The EDS X-ray elemental maps (Fig. 5) highlighted an enrichment of Si and Al and a depletion of Fe, Ni and Co in areas characterized by strong weathering effects (edges of the fragment).

3.2. Analysis of fragment 2

The DP-μLIBS averaged spectra in the spectral window 335–365 nm obtained on fragment 2 (Fig. 6) showed the emission lines of Fe, Ni and Co, whereas those of Al, Ca, Mg, Si and Li were absent. These findings confirmed the optical observation that this fragment was not altered and contaminated by terrestrial weathering.

The punctual analyses by DP-μLIBS were performed on dark and light thin lamellae as observed under microscope (Fig. 2b). The results obtained showed that the contents of Co and Ni were very different on the different spots analyzed, which might be likely ascribed

to the alternance of kamacite and taenite lamellae (Table 2). The plasma parameter (N_e and T_{ex}) values calculated from the spectra acquired on fragment 2 were similar to those obtained for fragment 1, which confirmed similar operational conditions of the instrumental apparatus and the similarity of the matrix.

Although in some cases a lack of Co was observed, as confirmed also by EDS-SEM analysis (Fig. 7, Table 3), the average content of Co was in the range of 0.2–1 wt%, i.e. the typical range found in iron meteorites [25]. The inomogeneous concentration of Co and Ni might be related to the plessite texture observed by optical microscopy and to a fine intergrowth of lamellae of taenite and kamacite observed by SEM (Fig.7).

The quantitative analytical data obtained by DP-μLIBS and confirmed by EDS-SEM indicated that an increase of Ni corresponded to a decrease of Co. The Co and Ni distribution in kamacite and taenite was used previously to evaluate the cooling rates of the iron meteorites of the IVA and IIIB group and mesosiderites [26]. Although the Dronino meteorite was classified in the ungrouped iron meteorites, its composition in the diagram Co/Ni fell into two groups, i.e. IVA and IAB [27,28]. Thus, the simultaneous quantitative variations of Ni and Co observed in this study were in substantial agreement with the data of Goldstein et al. [26] for the IVA-group iron meteorites. This finding might be explained by a solid-state diffusion process, i.e. during cooling Co diffused out of taenite into kamacite, while Ni behaved in the opposite way. Goldstein et al. [26] proposed that a decrease of the cooling rate might cause a greater increase of Co in kamacite associated to a corresponding decrease of Co in taenite. Further, the solid-state inverse diffusion of Co and Ni might also explain the formation of the observed plessite texture.

The X-ray elemental maps obtained by EDS-SEM on a small area of fragment 2, which contained also a portion of one of the elongated inclusions observed optically (red circle of Fig. 2b), revealed that the elongated inclusions corresponded to iron sulfides (green area in the S map in Fig. 8). Further, the maps of Fe, Ni and Co showed an inhomogeneous distribution at the microscale, which corresponded to the aggregation of kamacite and taenite.

These results confirmed the duplex structure of the Dronino meteorite, which consisted of an intimate intergrowth of kamacite and plessite (kamacite + taenite) [16]. However, differently from fragment 1, fragment 2 appeared to be enriched in taenite with respect to kamacite. Although LIBS and EDS-SEM represented different analytical approaches and used different spot sizes and amount of sample analyzed, data obtained by the two techniques showed a good agreement.
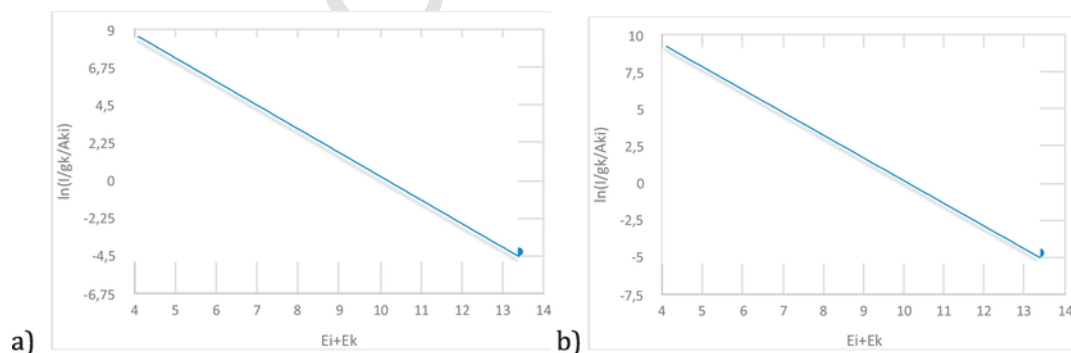

Fig. 4. Boltzmann plot of Fe emission lines for temperature calculation of fragment 1: a) polished, 7578 °K and b) unpolished, 8220 °K.

Table 1
Comparison of Fe, Ni and Co concentration data (average in wt%) obtained by CF-LIBS, EDS-SEM and EMPA analyses of the original and polished surfaces of fragment 1. The errors for LIBS data were calculated as standard deviation. The errors for SEM-EDS data correspond to the instrumental error.

Element	CF-LIBS polished surface	CF-LIBS original surface	EDS-SEM	EMPA[a] Kamacite	EMPA[a] Taenite
Fe	91.51±1.71	94.19±2.64	95.06±1.15	92.2	73.1
Ni	7.56±1.23	4.76±2.56	4.39±1.15	7±0.5	26.5±0.5
Co	0.93±0.64	1.06±0.10	0.56±0.20	0.75	0.35

[a] Reference data from Russell et al. [15].

3.3. Influence of the geo-pedological location on meteorite geochemistry

The analyses obtained in this study on the two fragments of the Dronino iron meteorite suggested that the two samples originated from two different environments, (i.e. a wet and a dry area). Actually, the two fragments were quite different not only in their optical features, but also in their chemical and mineralogical composition and texture. Fragment 1 was a weathered sample featuring a Fe, Ni and Co composition typical of kamacite in the unaltered portion of the polished section, whereas the presence of Al, Si, Ca, Mg, and Li indicated a more evident weathering toward the edges. These findings provided novel information on the geochemistry of weathering of Dronino meteorite, with respect to previous studies that revealed only the presence of secondary minerals formed by Fe oxidization, including maghemite, magnetite and goethite, and ferric hydrous oxides [16,17].

In particular, the presence of Si, Al Ca, Mg and Li allowed to evaluate the geochemical interactions occurred between the unweathered bulk meteorite and the geochemistry of the site. In these very last years, the interest in these studies was increasing in the attempt of distinguishing between the effects of terrestrial and pre-terrestrial weathering on mineral chemistry, and understanding the terrestrial geochemical processes leading to the formation of secondary miner-als. For example, LIBS data acquired on iron meteorites found on Mars raised a great attention in the evaluation of alteration processes that might affect their surfaces. This, in an attempt to assess weathering conditions on the Martian surface by comparing the external surface of iron meteorites on Mars with those found on the Earth [29].

Further, the DP-μLIBS technique associated with optical microscopy allowed to obtain data on the presence of specific microstructures occurring on the meteorite surface. For example, a different composition could be observed in Fig. 2b between the dark and light regions of the particular microstructure. In particular, the dark ones were composed of kamacite and the light ones of a Ni-rich iron phase or phases (kamacite+plessite). The different mineralogical composition of fragment 1 (kamacite) and fragment 2 (mainly taenite) could be related to a different state of weathering suffered by the two samples. The quantitative CF-LIBS data obtained for Fe, Ni and Co indicated a depletion of Ni as the alteration increased (Table 1). The correlation between the lower content of Ni and the terrestrial alteration due to weathering processes was previously observed and studied on the Wolf Creek iron meteorite [30,31]. Similar to findings of this study, these authors found that the weathered samples contained less Ni than the original meteorites, which led to the hypothesis that a considerable part of Ni would have been carried away in solution during the weathering process.

In agreement with the studies mentioned above, the loss of Ni during the alteration could be explained by the different water solubility of Ni and Fe at various pHs. In aerated solutions Fe readily oxidized to the ferric state and precipitated as ferric oxides and hydroxides even at low pH (about 2–3), whereas Ni could oxidize beyond the bivalent state, thus it did not precipitate as Ni hydroxide up to about pH 7. Therefore, Ni was much more soluble than Fe in acidic weathering conditions, so it could be removed by the acidic circulating water in sites of active weathering. Similar conclusions were reached also by Zubkova et al. [32] who suggested that the Ni-Fe sulfate and Ni hexahydrite compounds found in the Dronino meteorite were formed by oxidation of kamacite in association with violarite (Fe, Ni sulfide).
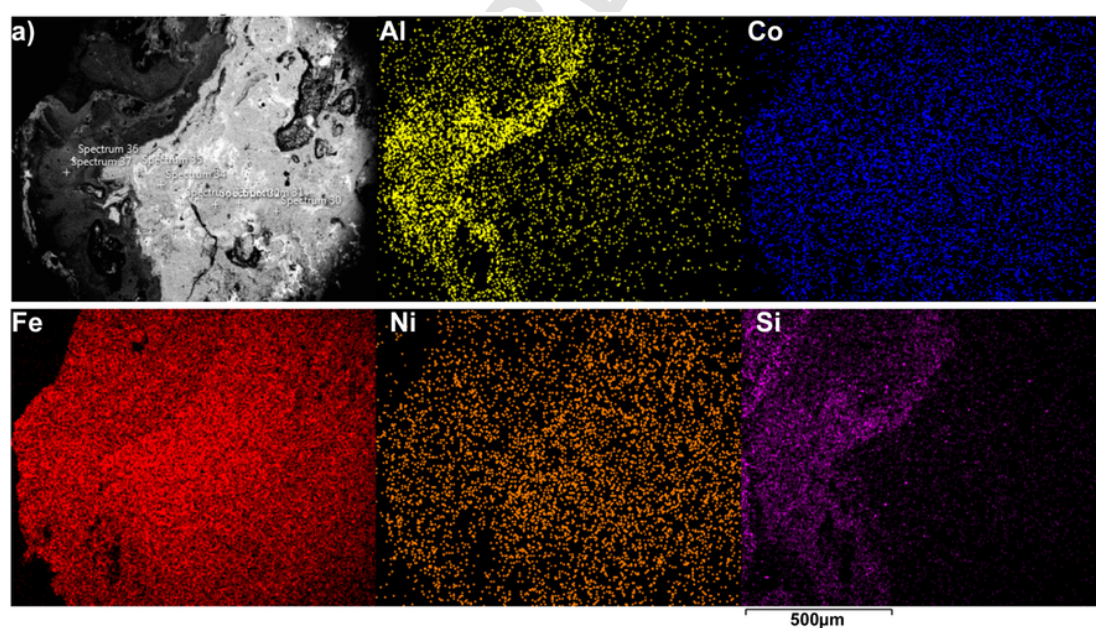

Fig. 5. SEM analyses of fragment 1. BSE image (a) and EDS elemental maps.
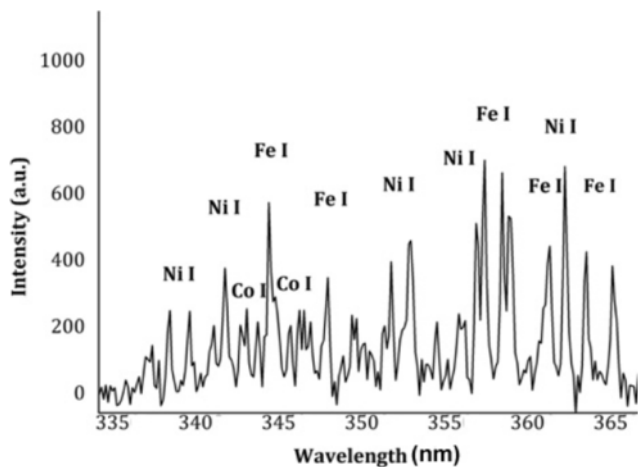
Fig. 6. DP-µLIBS spectrum of fragment 2 in the spectral window 335–365 nm.

Table 2
Comparison of Fe, Ni and Co concentration values (wt%) obtained by CF-LIBS. P1 and P5 represented the spots analyzed (see Fig. 2b) on fragment 2. The errors correspond to standard deviation.

Element	P1	P5
Fe	92.30 ± 1.56	80.54 ± 1.44
Ni	7.14 ± 1.74	19.46 ± 1.85
Co	0.56 ± 0.21	0

4. Conclusions

Results of this work confirmed the suitability of DP-µLIBS to analyze the compositional and mineralogical characteristics of iron meteorites. In particular, DP-µLIBS equipped with optical microscope permitted to distinguish fragments extensively weathered from those poorly weathered, so providing insights on the geochemistry of the sampling sites. The main difference between the two fragments analyzed was the presence of the elements Al, Ca, Mg, Li and Si only in the extensively weathered fragment 1. The presence of Al, Ca, Mg and Si was related to the typical minerals of clays and sands. The pervasive presence of Li, which was never reported so far in Dronino meteorite, likely due to the lack of detectability of light elements by other routinary techniques, was feasibly ascribed to contamination by alkaline-rich fluids occurring in the swamps in which fragment 1 was found. The different degree of terrestrial alteration between the fragments was confirmed also by their different mineralogical composition, i.e. by kamacite (low Ni) as the main component of fragment 1 and by mainly taenite (high Ni) with some kamacite in fragment 2. The lower content of Ni on the surface of the altered fragment 1 was ascribed to the effects of acidic weathering that caused the removal of bivalent Ni.

Further, DP-µLIBS combined with optical microscope was confirmed to be a promising analytical technique for investigating the relationships existing between microstructures and compositions of iron meteorites and their cooling rates. In particular, CF-LIBS data obtained by punctual analyses of the plessite texture found on the unaltered sample (fragment 2), confirmed its typical inhomogeneous mineralogical and chemical composition. Finally, the local and associated variability of Ni and Co (increase of Ni and decrease of Co and vice-versa) suggested the occurrence of solid state diffusion processes under a slow cooling rate in the Dronino meteorite.
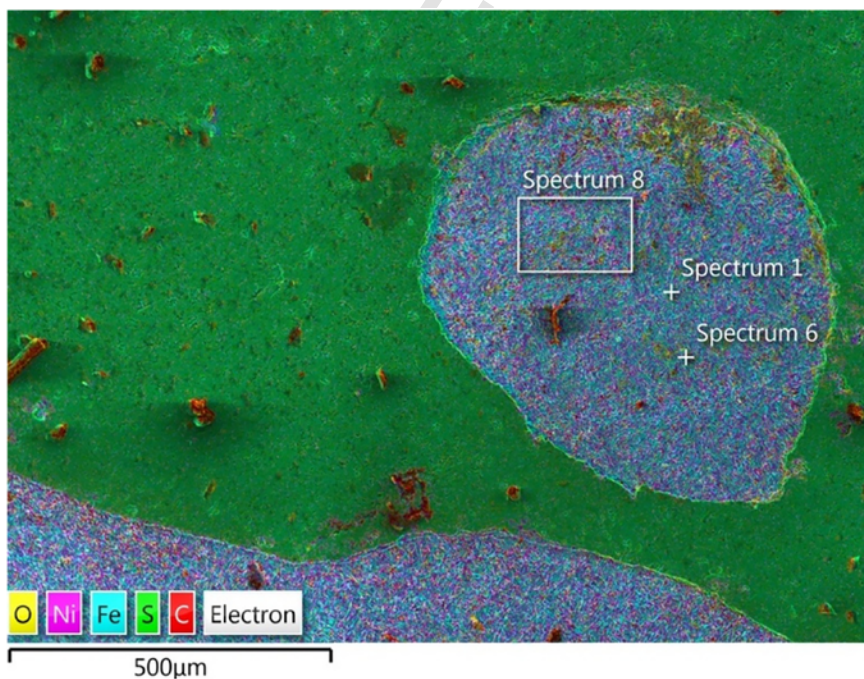
Fig. 7. SEM-EDS layered image of fragment 2. Spectrum 1 (Sp1) and 6 (Sp6) represent point analyses. Spectrum 8 (Sp8) is a raster analysis of the rectangular area. The corresponding data are shown in Table 3.

Table 3
Comparison of Fe, Ni and Co concentration values (wt%±instrumental errors) acquired by SEM-EDS analyses on Sp1, Sp6 and Sp8 sites on fragment 2 shown in Fig. 7.

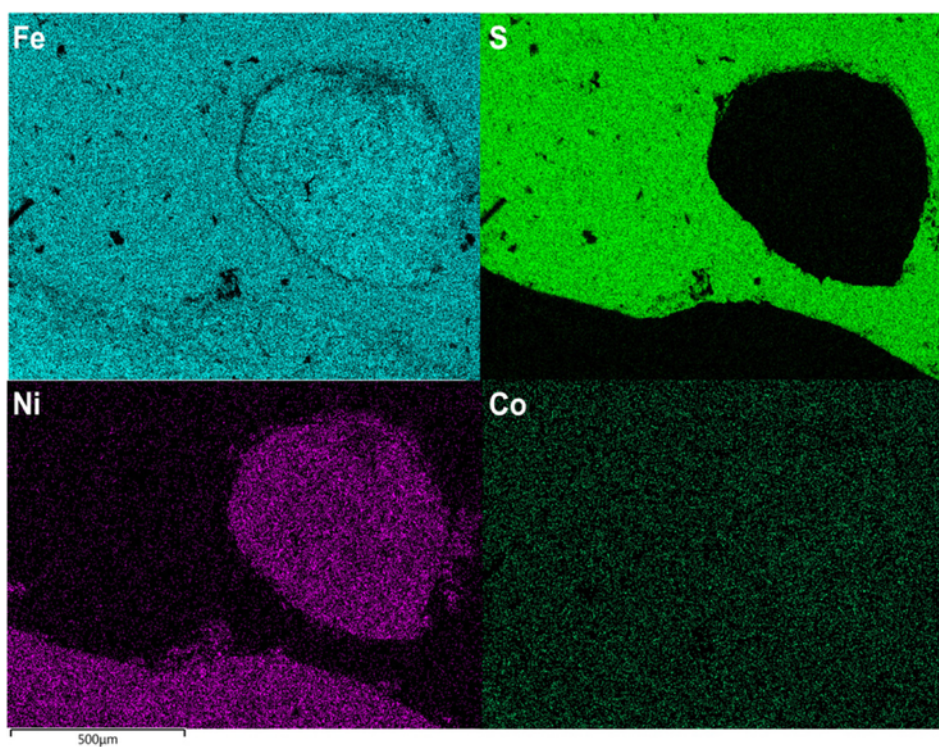| Element	Sp1	Sp6	Sp8
Fe	69.83±1.15	90.70±1.15	74.93±1.15
Ni	30.17±1.15	8.19±1.15	24.27±1.15
Co	0	1.10±0.20	0.80±0.20

Fig. 8. SEM-EDS X-ray elemental maps taken on the same area shown in Fig. 7.

References

[1] G.K. Benedix, H. Haack, T.J. McCoy, Iron and stony-iron meteorites, in: A.M. Davis (Ed.), Meteorites and Cosmochemical Processes, Vol. 1 of Treatise on Geochemistry, second ed.Elsevier, Amsterdam, 2014, pp. 267–285.

[2] D.A. Cremers, L.J. Radziemski, Handbook of Laser-Induced Breakdown Spectroscopy, second ed., John Wiley & Sons, Chichester, 2006.

[3] F.J. Fortes, J.J. Laserna, The development of fieldable laser-induced breakdown spectrometer: no limits on the horizon, Spectrochim. Acta B 65 (2010) 975–990.

[4] R.S. Harmon, R.E. Russo, R.R. Hark, Applications of laser-induced breakdown spectroscopy for geochemical and environmental analysis: a comprehensive review, Spectrochim. Acta B 87 (2013) 11–26.

[5] G.S. Senesi, Laser-Induced Breakdown Spectroscopy (LIBS) applied to terrestrial and extraterrestrial analogue geomaterials with emphasis to minerals and rocks, Earth Sci. Rev. 139 (2014) 231–267.

[6] R.C. Wiens, S. Maurice, B. Barraclough, M. Saccoccio, W.C. Barkley, J.F. Bell III, S. Bender, J. Bernardin, D. Blaney, J. Blank, M. Bouyé, N. Bridges, N. Bultman, P. Caïs, R.C. Clanton, B. Clark, S. Clegg, A. Cousin, D. Cremers, A. Cros, L. DeFlores, D. Delapp, R. Dingler, C. D'Uston, M. Darby Dyar, T. Elliott, D. Enemark, C. Fabre, M. Flores, O. Forni, O. Gasnault, T. Hale, C. Hays, K. Herkenhoff, E. Kan, L. Kirkland, D. Kouach, D. Landis, Y. Langevin, N. Lanza, F. LaRocca, J. Lasue, J. Latino, D. Limonadi, C. Lindensmith, L. Little, N. Mangold, G. Manhes, P. Mauchien, C. McKay, E. Miller, J. Mooney, R.V. Morris, L. Morrison, T. Nelson, H. Newsom, A. Ollila, M. Ott, L. Pares, R. Perez, F. Poitrasson, C. Provost, J.W. Reiter, T. Roberts, F. Romero, V. Sautter, S. Salazar, J.J. Simmonds, R. Stiglich, S. Storms, N. Striebig, J.J. Thocaven, T. Trujillo, M. Ulibarri, D. Vaniman, N. Warner, R. Waterbury, R. Whitaker, J. Witt, B. Wong-Swanson, The ChemCam instrument suite on the Mars Science Laboratory (MSL) rover: body unit and combined system tests, Space Sci. Rev. 170 (2012) 167–227.

[7] J.R. Thompson, R.C. Wiens, J.E. Barefield, D.T. Vaniman, H.E. Newsom, S.M. Clegg, Remote laser induced breakdown spectroscopy analyses of Dar al Gani 476 and Zagami Martian meteorites, J. Geophys. Res. 111 (2006), E05006.

[8] A. De Giacomo, M. Dell'Aglio, O. De Pascale, S. Longo, M. Capitelli, Laser induced breakdown spectroscopy on meteorites, Spectrochim. Acta, Part B 62 (2007) 1606–1611.

[9] M. Dell'Aglio, A. De Giacomo, R. Gaudiuso, O. De Pascale, G.S. Senesi, S. Longo, Laser induced breakdown spectroscopy applications to meteorites: chemical analysis and composition profiles, Geochim. Cosmochim. Acta 74 (2010) 7329–7339.

[10] A. Cousin, V. Sautter, C. Fabre, S. Maurice, R.C. Wiens, Textural and modal analyses of picritic basalts with ChemCam Laser-Induced Breakdown Spectroscopy, J. Geophys. Res. 117 (2012), E10002.

[11] J. Plavčan, M. Horňáčková, Z. Grolmusová, M. Kociánová, J. Rakovský, P. Veis, Sikhote-Alin meteorite, elemental composition analysis using CF LIBS, In: WDS 12 Proceedings of Contributed Papers, Part II, 2012, pp. 123–127.

[12] M. Horňáčková, J. Plavčan, J. Rakovský, V. Porubčany, D. Ozdin, P. Veis, Calibration-free laser induced breakdown spectroscopy as an alternative method for found meteorite fragments analysis, Eur. Phys. J. Appl. Phys. 66 (2014), 10702.

[13] G.S. Senesi, G. Tempesta, P. Manzari, G. Agrosì, An innovative approach to meteorite analysis by laser-induced breakdown spectroscopy, Geostand. Geoanal. Res. 40 (4) (2016) 533–541.

[14] V.I. Grokhovsky, V.F. Ustyugov, D.D. Badyukov, M.A. Nazarov, Dronino: An ancient iron meteorite shower in Russia, In: 36th Annual Lunar and Planetary Science Conference, March 14-18 in League City, Texas, 2005, (abstract no. 1692).

[15] S.S. Russell, L. Folco, M.M. Grady, M.E. Zolensky, R. Jones, K. Righter, J. Zipfel, J.N. Grossman, The meteoritical bulletin, No. 88, 2004 July, Meteorit. Planet. Sci. 39 (8) (2004) A215–A272, (Supplement).

[16] V.I. Grokhovsky, M.I. Oshtrakh, O.B. Milder, V.A. Semionkin, R.M. Kadushnikov, S.A. Glazkova, Structural studies of iron meteorite Dronino, In: 36th Annual Lunar and Planetary Science Conference, March 14-18 in League City, Texas, 2005, (abstract no.1980).

[17] G.A. Yakovlev, A.V. Chukin, V.I. Grokhovsky, V.A. Semionkin, M.I. Oshtrakh, Study of Dronino iron meteorite weathering in clay sand using Mössbauer spectroscopy, Croat. Chem. Acta 89 (1) (2016) 117–124.

[18] A. Ciucci, M. Corsi, V. Palleschi, S. Rastelli, A. Salvetti, E. Tognoni, New procedure for quantitative elemental analysis by laser-induced plasma spectroscopy, Appl. Spectrosc. 53 (1999) 960–964.

[19] G. Cristoforetti, A. De Giacomo, M. Dell'Aglio, S. Legnaioli, E. Tognoni, V. Palleschi, N. Omenetto, Local thermodynamic equilibrium in laser-induced breakdown spectroscopy: beyond the McWhirter criterion, Spectrochim. Acta B 65 (2010) 86–95.

[20] J.L. Pouchou, F. Pichoir, A simplified version of the "PAP" model for matrix corrections in EPMA, in: D.E. Newbury (Ed.), Microbeam Analysis, San Francisco Press, 1988, pp. 315–318.

[21] J.L. Pouchou, F. Pichoir, Quantitative analysis of homogeneous or stratified microvolumes applying the model "PAP", in: K.F.J. Heinrich, D.E. Newbury (Eds.), Electron Probe Quantitation, Plenum Press, New York, 1991, pp. 31–75.

[22] https://www.nist.gov/pml/atomic-spectra-database.

[23] P.B. Tomascak, G.N. Hemming, S.R. Hemming, The lithium isotopic composition of waters of the Mono Basin, California, Geochim. Cosmochim. Acta 67 (2003) 601–611.

[24] N. Zhen, B. Lingzhong, Z. Mianping, Lithium resources industrialization of salt lakes in China: a case study of the Xitaijinaier salt lake and the Zabuye salt lake, Acta Geosci. Sin. 31 (2010) 95–101.

[25] B.H. Mason, M. Fleischer, Data of Geochemistry: Cosmochemistry. Meteorites, Parts 1–2, U.S. Department of the Interior, Geological Survey, 1979.

[26] J.I. Goldstein, J. Yang, E.R.D. Scott, Determining cooling rates of iron and stony-iron meteorites from measurements of Ni and Co at kamacite–taenite interfaces, Geochim. Cosmochim. Acta 140 (2014) 297–320.

[27] E.R.D. Scott, Chemical fractionation in iron meteorites and its interpretation, Geochim. Cosmochim. Acta 36 (1972) 1205–1236.

[28] M. Gemelli, M. D'Orazio, L. Folco, Chemical analysis of iron meteorites using a hand-held X-ray fluorescence spectrometer, Geostand. Geoanal. Res. 39 (2014) 55–69.

[29] N.L. Lanza, P.J. Gasda, A.M. Ollila, R.C. Wiens, S.M. Clegg, D. Delapp, M. Bodine, C. Agee, P.-Y. Meslin, P. Beck, H.E. Newsom, S. Maurice, Analyzing natural meteorite exteriors with laboratory LIBS for comparison to meteorites encountered by Curiosity in Gale Crater, Mars, In: 80th Annual Meeting of the Meteoritical Society, LPI Contrib. n. 1987, 2017, (Abstract#6402).

[30] J.S. White, E.P. Henderson, B. Mason, Secondary minerals produced by weathering of the Wolf Creek meteorite, Am. Mineral. 52 (1967) 1190–1197.

[31] M.R. Lee, P.A. Bland, Mechanisms of weathering of meteorites recovered from hot and cold deserts and the formation of phyllosilicates, Geochim. Cosmochim. Acta 68 (2004) 893–916.

[32] N. Zubkova, I. Pekov, N. Chukanov, P. Dmitry, S. Kazantsev, Nickelhexahydrite from the weathered meteorite Dronino: variations of chemical composition, crystal structure, and genesis, Dokl. Earth Sci. 422 (2008) 1109–1112.